Influence of disorder on the photoinduced excitations in phenyl substituted polythiophenes

Christoph J. Brabec,[a] Christoph Winder, Markus C. Scharber, and N. Serdar Sariciftci
Christian Doppler Laboratory for Plastic Solar Cells at the Linz Institute for Organic Solar Cells (LIOS), Physical Chemistry, Johannes Kepler University Linz, A-4040 Austria

Jan C. Hummelen
Stratingh Institute and Materials Science Center, University of Groningen, 9747 AG Groningen, The Netherlands

Mattias Svensson and Mats R. Andersson
Chalmers University of Technology, Department of Polymer Technology and Organic Chemistry, Gothenburg, Sweden

(Received 9 January 2001; accepted 30 July 2001)

Regioregular poly(3-(4′-(1″,4″,7″-trioxaoctyl)phenyl)thiophenes) (PEOPTs) exhibit interesting properties for the use in polymer electronics. Exposing thin films of the amorphous, disordered phase (orange phase) of the ''as prepared'' polymer to chloroform vapor or annealing them by heat treatment results in a redshift of the absorption maximum due to the formation of nanocrystals in an ordered phase (blue phase). As such, PEOPT thus is a very interesting conjugated polymeric material, which exhibits two different phases with well-defined order/disorder characters on one-and-the-same material. This property opens up the unique possibility to investigate the role of order/disorder on the photoexcited pattern without being obscured by the differences in chemical structure by using different materials with different crystallinity. The fact, that blue phase PEOPT exhibits absorption edges at relatively low energies around 1.8 eV, thereby demonstrating an enhanced spectral absorption range as compared to the orange phase, makes them attractive for use in photodiodes and solar cells as well. The photoinduced charge generation efficiency in both phases of PEOPT is significantly enhanced by the addition of a strong electron acceptor such as fullerene C_{60}, as observed by quenching of the luminescence and by photoinduced absorption measurements in the infrared and uv–visible regime. The average number and the lifetime of photoinduced carriers in composites of PEOPT with a methanofullerene [6,6]-phenyl C_{61}–butyric acid methyl ester (PCBM) are found to depend on the crystallinity of PEOPT in thin films, which gives rise to charged photoexcitations delocalized between polymer chains. Stronger bimolecular recombination in composites of the blue phase PEOPT with PCBM is observed as compared to the orange phase PEOPT/PCBM films. The origin of this enhanced recombination is found to be related to the hole mobility of the polymer. © *2001 American Institute of Physics.* [DOI: 10.1063/1.1404984]

I. INTRODUCTION

Polythiophenes are a very versatile class of conjugated polymers. Substituted polythiophenes were among the first conjugated polymers modified by attaching long solubilizing side chains to improve their solubility and processability.[1] Substituted polythiophenes can be tailored for various applications by designing the side groups to give the polymer different properties. Especially for device applications, polythiophenes have several attractive properties: They are relatively stable and the monomer synthesis is easy and versatile. This easy synthesis allowed researchers to develop polythiophenes that were tested successfully for electroluminescent diodes emitting in the whole visible spectral range,[2] for optically pumped lasing,[3] for organic transistors,[4] and recently also for photodiodes[5] and solar cells.[6] For some processable polythiophenes, among them the poly(3-alkylthiophenes), a thermochromic change between an orange and a blue phase[7] was reported. The origin of this thermochromism was extensively studied from a structural point of view especially with respect to the interplay between the effective conjugation length of the thiophene backbone and the conformational change of the alkyl side chains (i.e., flat *trans* versus twisted *gauche* structures).[8–10]

Recently, emphasis was put again on the investigation of the two different phases in substituted polythiophenes, demonstrating a photoinduced phase transformation in polyalkylthiophenes within the nanosecond regime.[11] The regioregularity of the polythiophenes has an important influence on the effective conjugation length. For regioregular thiophenes, the π conjugation seems to be longer since the thiophene rings are less twisted relative to each other due to decreased steric hindrance.[12]

For a series of regioregular substituted poly(3-phenylthiophenes) this phenomena of two different phases was studied extensively by x-ray diffraction.[13,14] In general, the class of substituted poly(3-phenylthiophenes) is semi-

[a]Electronic address: christoph.brabec@jk.uni-linz.ac.at

crystalline. A highly interesting phenomena is observed for many of the poly(3-phenylthiophenes) with a para substitution of the phenyl ring. Depending on the processing conditions, spin-coated thin films of these polymers can exist in two distinct states with different crystallinity: a less crystalline state with a larger spacing of the highest occupied–lowest unoccupied molecular orbital (HOMO–LUMO) distance and a higher crystalline state with a lower HOMO–LUMO distance.[13] The general trend observed was that poly(3-phenylthiophenes) initially go into a metastable, poorly crystalline state in the ''as-prepared'' form and then achieve a thermodynamically more stable form after appropriate treatment. These two phases are subsequently referred to as orange phase (lower crystallinity) and blue phase (higher crystallinity), indicating their different colors. The poly(3-phenylthiophenes) with para-substituted phenyl rings have structures in which the substituted side chains are directed away from the polymer backbone. The main chains therefore pack closer along the *b* axis but are spaced with longer distances along the *a* axis. According to the x-ray studies the packing of the chains to each other is higher in the blue phase compared to the orange phase.[14] Exposing thin films of the amorphous, disordered phase (orange phase) of the ''as-prepared'' polymer to chloroform vapor at room temperature or annealing them by heat treatment results in a redshift of the absorption maximum due to the formation of more and larger nanocrystals in an ordered phase (blue phase).

As such, poly(3-(4′-(1″,4″,7″-trioxaoctyl)phenyl)thiophene) (PEOPT) thus is a very interesting conjugated polymeric material, which exhibits two different phases with well-defined order/disorder character on one-and-the-same material. This property opens up the unique possibility to investigate the role of order/disorder on the photoexcited pattern without being obscured by the differences in chemical structure by using different materials with different crystallinity. Further interest in these regioregular polythiophenes stems from enhanced absorption in the near-infrared regime, which makes this class of polymers an interesting candidate for solar cell device applications because the polymers will absorb more of the terrestial solar spectrum due to their low band gap. Since the discovery of an ultrafast photoinduced electron transfer[15] from many conjugated polymers to fullerenes, this effect has been used to enhance the quantum efficiency for charge generation and thereby also the photovoltaic performance of conjugated polymers.[16–19]

In this paper we investigate the quasi-steady-state photoexcitations of a special representative of the class of regioregular phenyl-substituted polythiophenes,[2,5,20] PEOPT, in its pristine state as well as in composites with and without fullerenes. The influence of the degree of disorder of these two phases of poly(3-phenylthiophenes) on the photoexcitation pattern as well as on the occurrence of photoinduced charge transfer to fullerenes is studied and their relative potential in photovoltaic applications is evaluated.

II. EXPERIMENT

The chemical structure of PEOPT (Ref. 21) and [6,6]-phenyl C_{61}–butyric acid methyl ester (PCBM) (Ref. 22) as well as the investigated device structure is shown in Fig. 1. The enhanced solubility of PCBM compared to C_{60} allows a high fullerene-conjugated–polymer ratio and strongly supports the formation of donor–acceptor bulk heterojunctions.

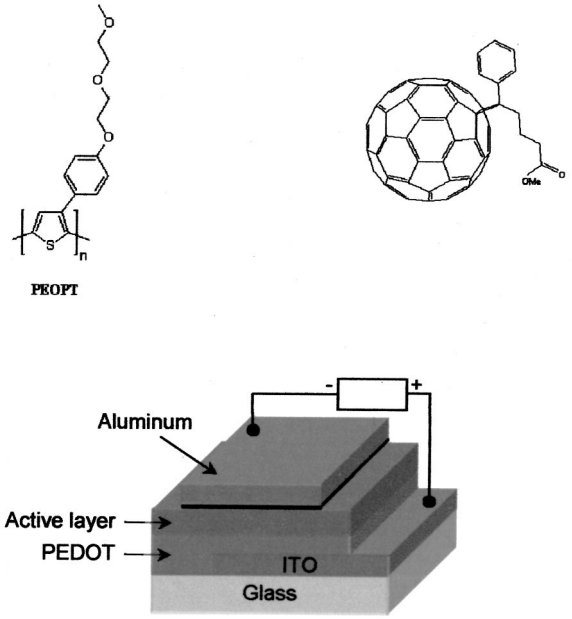

FIG. 1. Chemical structure of PEOPT and PCBM and solar cell device structure.

Orange phase thin-film samples were produced by spin casting from 1 to 1.5 wt % solutions of PEOPT in chloroform at high spinning speed. The conversion of the orange phase cast films to the blue phase can be performed by either a temperature step of ~100 °C for 10 min or by exposing the films directly after spin casting to chloroform vapor at room temperature. Casting PEOPT from orthodichlorobenzene (ODCB) solutions or from mixtures of chloroform with toluene directly results in thin films in the blue phase. The results on the blue phase presented in this study were obtained by spin-casting films from chloroform/toluene 1:1 mixtures except for the pristine blue PEOPT diode, which was converted by a temperature step.

Photoinduced absorption (PIA) measurements were performed at liquid-nitrogen temperature under a vacuum better than 10^{-3} Pa as described elsewhere.[23] Devices with an active area of 5 mm^2 were produced between ITO/PEDOT:PSS (indium tin oxide)/(poly(3,4-ethylenedioxythiophene)-poly(styrenesulfonate) substrates and thermally evaporated Al electrodes. The photoactive layer consisting of pristine PEOPT was spin-coated from 1% chloroform solution to a thickness of less than 100 nm. Conversion of the orange to the blue phase was performed by a temperature step of 100 °C for 10 min. Bulk heterojunction devices with fullerenes were produced with the same technology, but different geometry. Since the devices were aimed for PIA measurements, a large-area semitransparent top electrode is needed and the appropriate active area of the devices was ~1 cm^2. Thin films were spin-cast from 1:1 ratios of PCBM-:PEOPT from chloroform (orange phase) or chloroform/toluene (blue phase) solutions. The aluminum top electrode

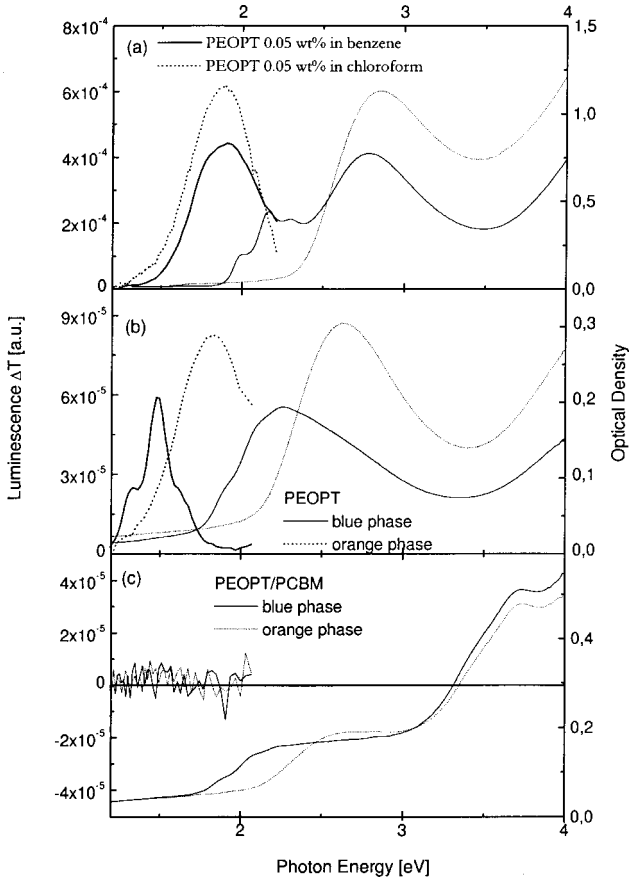

FIG. 2. Right axis: uv–visible absorption of the two phases of PEOPT in solution and in the solid state, with and without fullerenes, (a) PEOPT in 0.05 wt % solutions in chloroform (dotted line) and benzene (continuous line). (b) uv–visible absorption spectra of PEOPT spin-cast films, orange (dotted line) and blue phase (continuous line). (c) uv–visible absorption spectra of PEOPT/PCBM 1:1 mixtures, spin cast, PEOPT in blue (continuous line) and orange phase (dotted line). Left axis: Luminescence spectra of the two phases of PEOPT in solution and in the solid state, with and without fullerenes. (a) Luminescence of PEOPT in 0.05 wt % solution in chloroform (dotted line, divided by a factor of 5 for better comparison) and benzene (continuous line) at 298 K. (b) Luminescence of PEOPT spin-cast films at 80 K, orange (dotted line) and blue phase (continuous line). (c) Luminescence of PEOPT/PCBM composite spin-cast films at 80 K, orange (dotted line) and blue phase (continuous line).

was thermally evaporated with a thickness of 15 nm. Photocurrents were measured at room temperature in vacuum. Illumination through the transparent ITO side was done by white light from a halogen lamp with 60 mW/cm^2. $I-V$ curves were recorded with a Keithley 2400 source meter, typically by averaging 200 measurements for one point. Spectrally resolved photocurrent measurements were recorded by a lock-in technique, illuminating the device with $\sim$0.1 mW/cm^2 monochromatized light from a Xe arc lamp and white light background illumination. Light intensities were measured by a calibrated Si photodiode.

III. RESULTS AND DISCUSSION

A. Absorption and luminescence

1. Solution

The solution absorption spectra of PEOPT in benzene and chloroform solutions are shown in Fig. 2(a). Both solutions show their maximum at 2.70 eV. The oscillator strength for peak absorption at 2.7 eV is higher for chloroform than for benzene. For benzene solutions of PEOPT, further peaks at 2.19, 2.02, and 1.83 eV are observed. The onset for the absorption in benzene solutions is around 1.70 eV, while for the chloroform solution the onset of absorption is observed at 2.15 eV. Comparing the absorption spectra to the solid-state film absorption [Fig. 2(b)], the high-energy peak at 2.7 eV is assigned to the orange phase, while the low-energy absorption features of the benzene solution at 2.19, 2.02, and 1.83 eV, which are absent in the chloroform solution, are assigned to the blue phase. Obviously, the absorption spectra in benzene is a mixture of the blue and orange phase, while in chloroform solution only the orange phase is observed. Qualitative results similar to those observed for benzene solutions were observed for solutions of PEOPT in chlorobenzene, dichlorobenzene, and toluene. In all these solvents both phases of PEOPT are observed, while chloroform is the only solvent giving the orange phase exclusively.

The luminescence of PEOPT in solution is plotted in Fig. 2(a) for chloroform and benzene as solvents. The luminescence in benzene shows a maximum at 1.89 eV; for the chloroform solution this maximum is observed at 1.86 eV. The emission in chloroform is almost an order of magnitude higher than the emission in benzene. Comparison of the solution luminescence with luminescence from thin solid films allows assignment of the emission to originate dominantly from photoexcitations in the orange phase. This is in agreement with recent reports that the luminescence quantum yield of blue phase PEOPT is considerably lower than that for orange phase PEOPT. The blue phase emission from PEOPT in these two solvents is therefore either absent or below the detection limit of the photomultiplier setup.

2. Thin films

Thin films of PEOPT were characterized by absorption, luminescence, and photoinduced absorption measurements. The absorption maximum of the orange phase films is observed at 2.63 eV while the onset is around 2.1 eV. For the blue phase films, the maximum is observed at 2.25 eV with the onset at 1.75 eV [Fig. 2(b)]. The blue phase has an additional shoulder at 1.92 eV. The huge shift of the onset for the absorption from 2.1 eV in the orange phase to 1.75 eV in the blue phase is assigned to a narrowing of the HOMO–LUMO levels. This narrowing of the HOMO–LUMO levels is also observed by fluorescence measurements at 80 K, plotted in Fig. 2(b). The orange phase shows a broad fluorescence peak with a maximum at 1.84 eV and a shoulder at 1.70 eV. The maximum of the fluorescence in the blue phase is redshifted to 1.48 eV.

Ultraviolet–visible light absorption spectroscopy was used to investigate the phase of PEOPT in composites with PCBM after processing and to ensure that PCBM does not hinder the structural reorganization of PEOPT from one phase to another. As shown in Fig. 2(c), both samples show an absorption feature around 3.5 eV that is attributed to the PCBM absorption. For the chloroform cast sample the onset of absorption is detected at the same position as for the pristine orange phase PEOPT thin films. Although the absorption

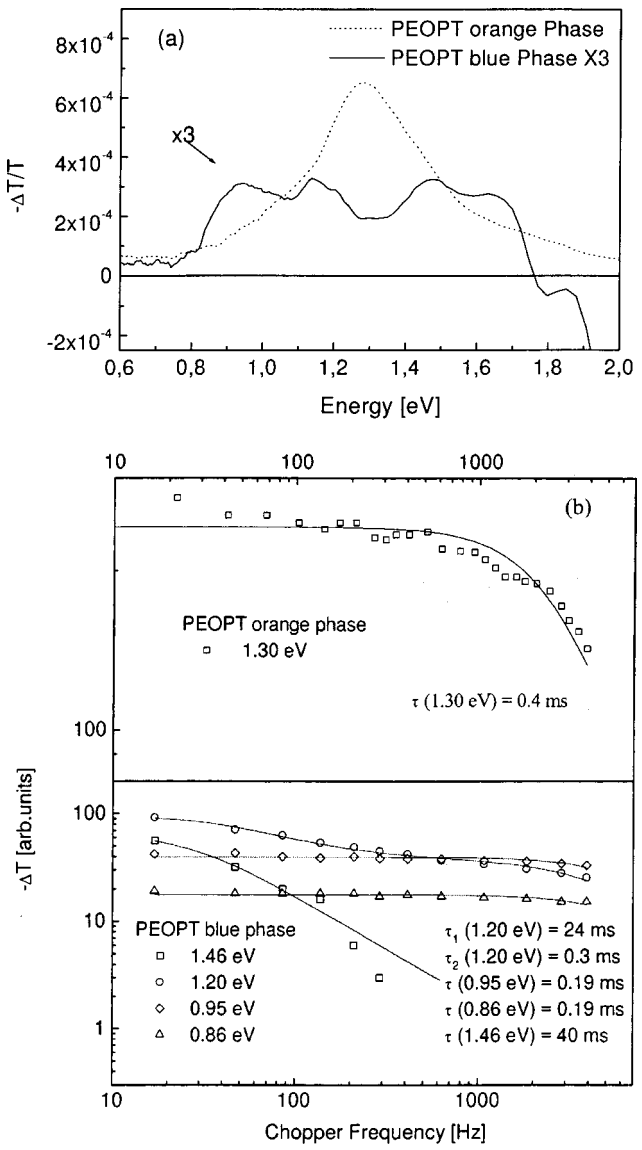

FIG. 3. (a) PIA spectra of PEOPT in the blue (continuous line) and orange phase (dotted line) at 80 K and 10^{-3} Pa, excitation at 488 nm with 150 mW laser power for the blue phase and 30 mW for the orange phase, chopper frequency 122 Hz. (b) Frequency dependence of the PIA features (ΔT) of PEOPT in the orange phase at 1.30 eV (open square, upper part) and for PEOPT in the blue phase at 1.46 eV (open square), at 1.20 eV (open circle), at 0.95 eV (open diamond), and 0.86 eV (open triangle) for PEOPT blue phase (lower part). The continuous lines are fits to a monomolecular decay model. The experimental conditions were as denoted in (a).

features at higher energies are partially hidden under the PCBM absorption, a maximum is observed at ~2.6 eV, which is again in good correlation with that of pristine orange phase PEOPT. The chloroform cast sample is therefore identified as orange phase PEOPT/PCBM composite. The onset of absorption of the chloroform/toluene cast sample is observed at 1.75 eV, which correlates with that of the pristine blue phase polymer. A smooth increase of absorption until 2.25 eV is followed by a flat plateau. Although the polymer peak absorption features are masked by the PCBM absorption, the blue and the orange phase samples are clearly identified by their different onset of absorption, which mirrors the different HOMO–LUMO levels. The ir absorption of PEOPT in composites with fullerenes is a linear superposition of the absorption spectra of the single components, and no signs of complex formation or ground-state charge-transfer complexes are observed.

TABLE I. Intensity scaling of PEOPT in various composites—excitation was done at 488 nm.

	Energy (eV)						
α (Compounds)	1.47	1.40	1.27	1.20	1.16	0.90	ir
Orange PEOPT			0.75				
Blue PEOPT	0.91			0.83		0.85	
Orange PEOPT/PCBM		0.37					0.45
Blue PEOPT/PCBM	0.40				0.40		0.39

Figure 2(c) shows the luminescence of the two composites with PCBM. Upon addition of PCBM the luminescence of the polymer is completely quenched (i.e., below the sensitivity of the setup), independent of the phase of the polymer, which is already indicative for the occurrence of photoinduced charge transfer.

B. Excited-state spectroscopy

Before presenting and discussing the experimental results of the pristine PEOPT and the PEOPT/PCBM composites we briefly review the effect of fullerene addition to nondegenerate ground-state conjugated polymers.[15,17,24–42] For many of the highly luminescent conjugated polymers (such as alkoxy-substituted PPVs) (poly phenylenevinylene) the dominant photoexcited absorption feature peak in the microsecond–millisecond time regime is attributed to a triplet–triplet absorption. Upon addition of fullerene several new features are observed in such composites: (i) nearly complete quenching of the luminescence accompanied by (ii) nearly complete quenching of the triplet state. Additionally (iii), long-lived new absorption features in the high-energy range (above the Fermi level) and in the low-energy range (below the Fermi level) are observed, assigned to the two dipole-allowed polaron transitions.[43]

The PIA spectra of the blue and orange phase thin films are compared in Fig. 3(a). For the orange phase one broad PIA feature is observed with a maximum at 1.27 eV. The intensity scaling of this feature scales with an exponent of 0.75, showing no signs of saturation even at monochromatic excitations intensities as high as 200 mW/mm^2 from the Ar^+ laser. Although the intensity scaling does not imply strict monomolecular recombination behavior (Table I), the fre-

TABLE II. Frequency scaling: Lifetimes are calculated with a monomolecular decay model for the pristine polymers and with a bimolecular decay model for polymer/PCBM mixtures.

τ (ms)	1.47	1.40	1.27	1.20	1.16	0.90	IR
Orange PEOPT			0.4				
Blue PEOPT	24			40		0.19	
				0.26			
Orange PEOPT/PCBM		4					2
		0.45					0.15
Blue PEOPT/PCBM	0.63				0.37		0.85
							0.08

quency dependence of the 1.27-eV feature was fitted to a first-order relaxation kinetics model (Table II) and a lifetime of 0.4 ms was obtained [Fig. 3(b)]. The photoexcitation pattern of the blue phase is more complex than that for the orange phase. Four PIA features are observed at 1.70 and 1.47 eV, one broader feature with two peaks around 1.20 eV, and one around 0.95 and 0.86 eV. While the signal intensity of the three features at higher energies scales with the excitation intensity with exponents α between 0.75 and 0.8, the low-energy feature at 0.86 eV scales with an exponent $\alpha = 0.9$ (Table I). The lifetimes of the PIA features were calculated by fitting a monomolecular recombination model (with up to two relaxation times) to the frequency dependence of the PIA signals. All the features show lifetimes in the millisecond range. The lifetime dependence of the 1.2-eV peak is more complicated and a monomolecular relaxation model with two lifetimes was necessary to receive a good fit.

The PIA of the composites of the orange phase PEOPT with PCBM (1:1 wt ratio) [Fig. 4(a), dashed line], shows a broad excited-state absorption feature between 1.2 and 2 eV with its maximum at around 1.40 eV. Additionally, a second PIA feature is observed at around 0.46 eV as shown in Fig. 5. Both absorption features show a laser power dependence with an exponent $\alpha \leqslant 0.5$ (Table I), which indicates a dominant bimolecular decay mechanism. The lifetimes of these features, as derived from fitting the frequency dependence of the single features [Fig. 4(b), Table II] to a second-order recombination kinetics (bimolecular recombination) are 0.15 and 4 ms. Again, two relaxation times were chosen to get a better fit.

The PIA of the blue phase PEOPT mixed with PCBM (1:1 wt ratio) [Fig. 4(a)] shows two high-energy absorption features at 1.47 eV (with an additional shoulder at 1.60 eV) and at 1.16 eV. Again, a low-energy feature is observed and spectrally fully resolved by the ir PIA measurements in Fig. 5. This low-energy feature shows a rather broad peak between 0.32 and 0.20 eV. The laser power dependence again reveals clearly a bimolecular decay mechanism (Table I); all peaks scale with $\alpha \cong 0.40$. The lifetimes were calculated from fits to the frequency dependence of the PIA features [Fig. 4(b)] with 0.37 and 0.85 ms. At very low energies (below 0.2 eV), infrared-activated vibrations (IRAVs) are observed. The photoexcited charges distort the polymer backbone lattice due to symmetry breaking as well as due to electron–phonon coupling. Therefore, upon photoexcitation totally symmetric Ag modes become infrared activated and result in appearance of these IRAV modes. The inset of Fig. 5 shows the fingerprint region of the IRAV of the two composites. Both composites, blue and orange PEOPT mixed with PCBM, show the same IRAV pattern.

The photoexcitation pattern of orange phase PEOPT with and without PCBM is similar to the scheme described above. Pristine orange PEOPT has only one long-lived photoexcitation in the high-energy range centered around 1.27 eV. No PIA features are found in the low-energy region down to 0.6 eV. Therefore, this photoexcitation is assigned to a triplet–triplet absorption. Upon addition of PCBM the emission of orange PEOPT and the triplet are strongly quenched and a novel high-energy photoinduced absorption feature

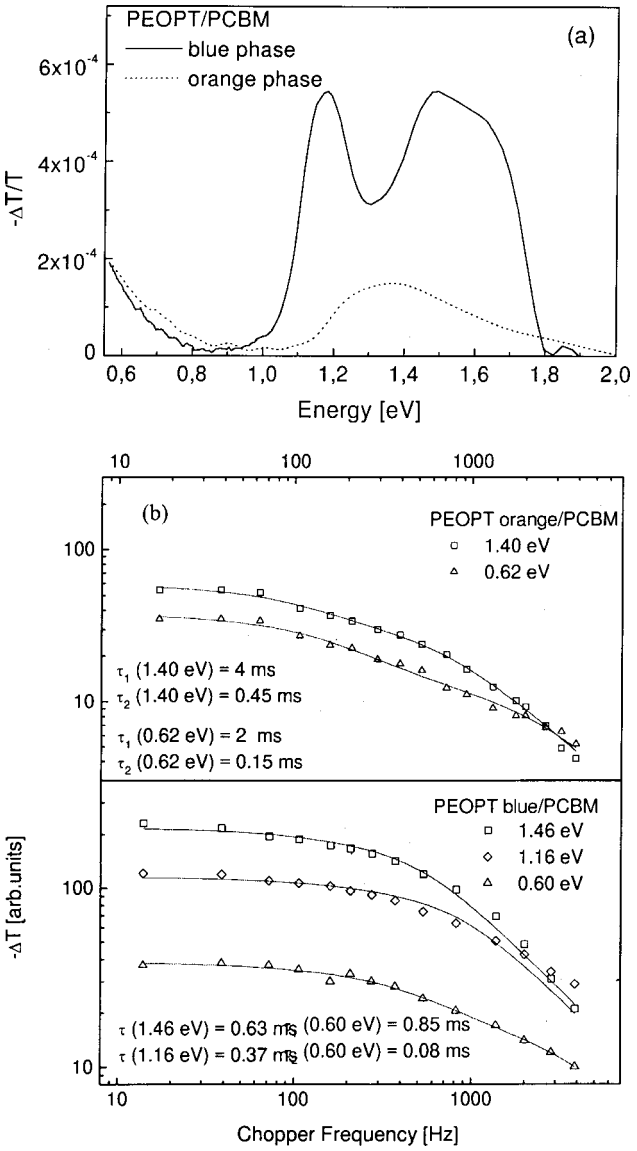

FIG. 4. (a) PIA spectra of PEOPT blue:PCBM 1:1 (continuous line) and PEOPT orange phase:PCBM 1:1 (dashed line) at 100 K and 10^{-3} Pa, excitation at 488 nm with 30 mW, chopper frequency 122 Hz. (b) Frequency dependence of the peaks (ΔT) at 1.41 eV (open square) and 0.62 eV (open triangle) for PEOPT in orange phase (upper part), at 1.46 eV (open circle), at 1.16 eV (open diamond), and 0.60 eV (open triangle) for PEOPT blue phase (lower part) and fit (continuous line); fit curve and lifetime are calculated for the bimolecular decay mechanism.

(HE1) is generated around 1.4 eV, as indicated by the different intensity and frequency scaling (listed in Table I). Additionally, a low-energy feature (LE1) with a maximum around 0.46 eV is generated. Both, the high- and the low-energy features follow the same scaling behavior and are identified as the low-energy and the high-energy polaron absorption bands of orange PEOPT.

The photoexcitation pattern of blue phase PEOPT is more complicated. For pristine blue phase PEOPT three different signals are observed, at 1.47 eV (with a high-energy shoulder at 1.65 eV), around 1.2 eV, and around 0.9 eV (Fig. 3, Tables I and II). The single excited-state absorption features are quite broad spectrally distributed and overlap with each other. Since the 0.9-eV peak can be quenched by the

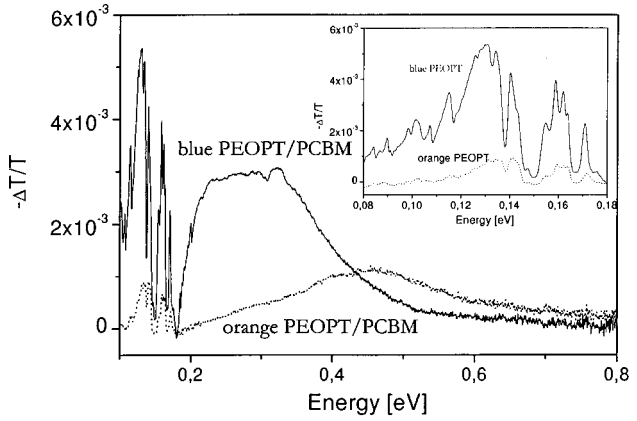

FIG. 5. Photoinduced absorption spectrum of blue PEOPT/PCBM (continuous line) and orange PEOPT/PCBM composites (dotted line) in the infrared region at 80 K. The inset is an enlargement of the IRAV region of the two samples.

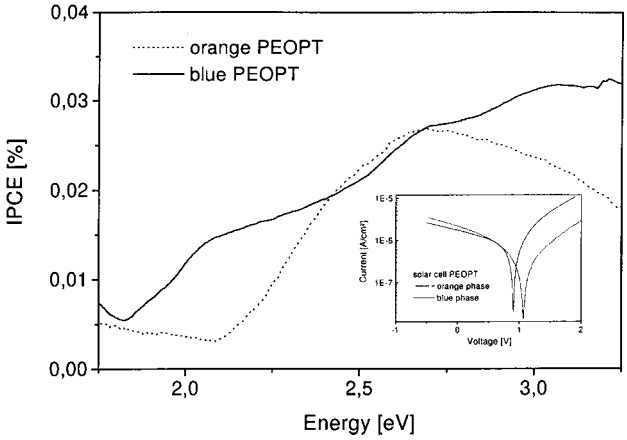

FIG. 6. Spectrally resolved photocurrent of blue PEOPT (continuous lines) vs orange PEOPT (dotted lines). The inset shows the $I-V$ curves under white light illumination with 60 mW/cm^2. Under these conditions, the following values were measured for the blue phase, $V_{oc}=0.91$ V, $I_{sc}=1.9\ \mu$A/cm^2, FF$=0.30$, and for the orange phase, $V_{oc}=1.06$ V, $I_{sc}=2.2\ \mu$A/cm, FF$=0.24$.

addition of fullerenes, it is suggested to assign this peak to the triplet–triplet absorption. The two peaks at 1.47 eV (HE2) and 1.2 eV (HE1) show very similar scaling behavior, indicating their common origin. In the blue phase PEOPT/PCBM composites two photoinduced absorption features are observed at high energies, at 1.5 eV (HE2) and at 1.18 eV (HE1). Additionally, a low-energy peak is observed with its peak around 0.25 eV (LE1). These three peaks scale similarly with laser intensity and chopping frequency. The HE1 and LE1 features are assigned to the high- and low-energy absorption features of photoexcited charged carriers (polarons) in blue PEOPT, respectively. The nature of the HE2 feature will be discussed below. It is interesting to note that the lifetime of the polarons in blue PEOPT is up to an order of magnitude shorter upon addition of PCBM and also considerably shorter than that in orange phase PEOPT/PCBM composites. Obviously, recombination of carriers is eased for blue phase PEOPT/PCBM composites, probably due to higher mobility of the carriers.

Due to the similar scaling behavior of the HE2 with the LE1 feature, the HE2 feature is supposed to originate from charged carriers; however, the energetic position does not fit the dipole-allowed polaron transitions.[44] Comparing the PIA features of blue and orange phase PEOPT/PCBM composites, it is evident that the low-energy features as well as the high-energy feature HE1 correspond to the same dipole-allowed transition of polarons in PEOPT, only shifted in energy due to the lowered HOMO–LUMO levels of the blue phase PEOPT. Therefore, the HE2 feature in blue phase PEOPT/PCBM, which follows the scaling behavior of the HE1 and features LE1 rather closely, has no pendant in the orange phase. For a chemically and electronically very similar polythiophene, poly[3-(4′-octylphenyl)thiophene] (POPT), which also shows comparable orange and blue phases, x-ray studies proved that the blue phase of this polymer has a considerable higher degree of crystallinity than the orange phase[13] and recent x-ray studies on PEOPT suggested the same trend.[14] In their blue phase the conformation of these polymers results in a much stronger interchain interaction (π stacking, aggregates) thereby causing the shift of the HOMO–LUMO levels. A similar phenomenon was observed recently for other regioregular polythiophenes.[45,46] In these polythiophenes, the formation of such two-dimensional lamellar structures induced increased interchain interactions that strongly influenced the traditional one-dimensional electronic properties of the polymer chains. These two-dimensional delocalized photoexcitations are characterized by their relatively small polaronic energy and by multiple absorption bands in the gap. Additionally it was found that in conformations without enhanced crystallinity the quantum efficiency of charge generation is considerably lower and neutral triplets are the dominant photoexcitations for polythiophenes. Following these reports[45,46] we interpret the PIA feature HE2 as a two-dimensional, delocalized charged photoexcitation induced by the interchain coupling in the blue phase of PEOPT. Such photoexcitations are expected to be absent in the unordered phase and are consequently not observed in the orange phase PEOPT.

C. PEOPT photodiodes: Conformation-induced change of the band gap

Thin-film photovoltaic devices were produced in order to investigate the spectral dependence of the photoinduced charge generation in the pristine polymer. Figure 6 shows the spectrally resolved photocurrent of blue PEOPT versus orange PEOPT. The measured photocurrent was transformed into the photovoltaic external quantum efficiency (collected charge carrier per incident photon) or the spectrally resolved incident photon to converted electron efficiency (IPCE) according to

$$\mathrm{IPCE}(\%)=[1240/\lambda(\mathrm{nm})]I_{sc}(\mu\mathrm{A/cm^2})/I_{inc}(\mathrm{W/m^2}), \quad (1)$$

where I_{inc} is the intensity of the incident light and λ the excitation wavelength. The maximum value of the IPCE for blue and orange PEOPT were found to be on the order of 5×10^{-2}%. The similar values of the IPCE for the both phases are mirrored in the magnitude of the short circuit current I_{sc} as seen from the $I-V$ curves of the diodes plotted

in the inset of Fig. 6. In general, the photodiodes from the pristine polymer showed very poor diode behavior with respect to rectification, and consequently the fill factors of the two diodes are low. Further, the diodes suffer considerably from large serial resistivities. The open circuit voltage of 0.91 and 1.06 V, respectively, for the orange and the blue phase are within the expectations for such diodes, taking into account the difference in the work functions ϕ_f of the anode (PEDOT: $\phi_f \sim 5.1\,\mathrm{eV}$) and the cathode (Al: $\phi_f \sim 4.3\,\mathrm{eV}$). The spectral shape of the IPCE of blue and orange PEOPT follows very closely the absorption spectra. The photodiodes from orange PEOPT show their photocurrent maximum at 2.7 eV and their onset at 2.1 eV. For blue PEOPT photodiodes the onset of photocurrent generation is observed at 1.8 eV, thereby ~0.3 eV redshifted compared to the orange phase PEOPT diodes.

The spectrally resolved photocurrent measurements for blue and orange phase PEOPT confirm the existence of two different confirmation-dependent band gaps of PEOPT as already indicated by the ground- and excited-state absorption measurements. Absorption and emission studies showed a narrowing of the HOMO–LUMO levels for the blue phase compared to the orange phase. Photoinduced absorption studies show that for the blue phase the position of the high-energy (HE1) and the low-energy (LE) polaron peaks are redshifted compared to the orange phase, each feature by ~0.15 eV. The narrowing of the HOMO–LUMO levels for the blue phase PEOPT is also indicated by the redshifted zero transition of the PIA signal. For blue phase PEOPT/PCBM this transition is observed at ~1.8 eV, while for red phase PEOPT/PCBM the transition is observed at ~2.1 eV.

The lowered onset of photocurrent for the blue phase justifies extension of the conclusions drawn for the HOMO–LUMO narrowing to the band gap of the polymer. Taking the results from absorption, emission, PIA, and photocurrent measurements together, it is therefore safe to conclude that blue phase PEOPT has an ~0.3 eV smaller band gap than the orange phase PEOPT. Since there are no chemical changes involved in the transition from the orange to the blue phase, the narrowing of the band gap has to have its origin in a conformational change of the polymer influencing the morphology and aggregation of chains.

D. Biased PIA on PEOTP/PCBM solar cells

In order to realize blue phase devices with film parameters comparable to the orange phase devices thin films were spin-cast from chloroform/toluene mixtures. Small amounts of toluene are enough to bring PEOPT into the blue phase, while chloroform guarantees the comparable film thickness as determined by α-stepper measurements. The $I-V$ curves for such devices recorded at room temperature are shown in the insets of Fig. 7(a). It is important to note that no optimization of the devices with respect to their efficiency was performed, regarding their film thickness, the semitransparent metal electrodes, the fullerene concentration, or the solvent used for spin casting. Therefore, the power characteristics of these devices, the I_{sc}, the V_{oc}, and consequently the power conversion efficiency η_{eff} are expected to become considerably higher for optimized devices.

Nevertheless, the photovoltaic devices show good diode behavior with rectification ratios of more than two orders of magnitude in the dark, making them suitable for field-induced PIA studies. Figure 7(a) shows the photoinduced absorption spectrum of two different devices at various operating conditions (under I_{sc}, and at -3 V). For the orange phase devices the field-dependent photoinduced absorption pattern consists of a broad absorption band with its maximum at ~1.4 eV, almost identical to the results from thin film measurements shown in Fig. 4(a). The spectral pattern of the PIA feature does not change upon applying voltage, and little dependency of the intensity of the PIA signal on the internally or externally applied field is observed. At -3 V the intensity of the PIA signal is enhanced by ~25%. For the blue phase device no or only a weak PIA signal was observed under short circuit conditions. Upon applying -3 V a broad PIA signal is clearly observed. The high-energy pattern of this PIA signal with two peaks at 1.45 and 1.8 eV may resemble the high-energy range of the thin-film PIA signal plotted in Fig. 4(a). The peak at 1.16 eV, observed for the blue PEOPT/PCBM film, is not resolved for the field-dependent PIA and only a broad absorption feature is observed at this position under external bias of -3 V. The intensity and frequency scaling behavior of the field-dependent PIA features, plotted in Figs. 7(b) and 7(c) respectively, indicate a bimolecular recombination mechanism for the excited-state absorption features in good correlation with the scaling behavior of the thin films. The relaxation kinetics of orange phase PEOPT/PCBM diodes is at least an order of magnitude slower than that for blue phase PEOPT/PCBM.

The PIA on blue and orange phase diodes give significant different signal amplitudes. For photoinduced absorption spectroscopy modulating the laser excitation with a mechanical chopper, only the long-lived carriers with a lifetime in the ms–sub-ms range are observed. Photoexcitations with a lifetime τ that are considerably larger than the inverse of the chopping frequency $1/\omega$ contribute to the PIA response with $1/\tau$, while photoexcitations with lifetimes shorter than $1/\omega$ contribute to τ. If no PIA is observed, either (i) the lifetime of the carriers (and thereby the average steady state concentration of carriers) is too low or (ii) the absorption cross section of the carriers is too low. We can exclude point (ii) to be responsible for the difference in signal amplitude between the orange and the blue phase, since the PIA measurements on thin films allowed us to observe the excited states for the blue and orange phase samples under comparable conditions. The frequency-dependent PIA measurements on blue phase PEOPT/PCBM revealed that the lifetime of charged carriers in blue phase PEOPT is considerably lower than that for orange phase PEOPT/PCBM.

Obviously, bimolecular recombination is more efficient in the blue phase of PEOPT compared to the orange phase. Under reverse bias, two effects can influence the amplitude of the PIA signal in photodiodes: (i) the lifetime can be changed due to a modified recombination process or (ii) the number of carriers in the sample can be enhanced due to higher quantum efficiency for charge generation[47] or reduced recombination. The difference in the lifetimes of the photodiode compared to the thin-film PIA signals is so small [Fig.

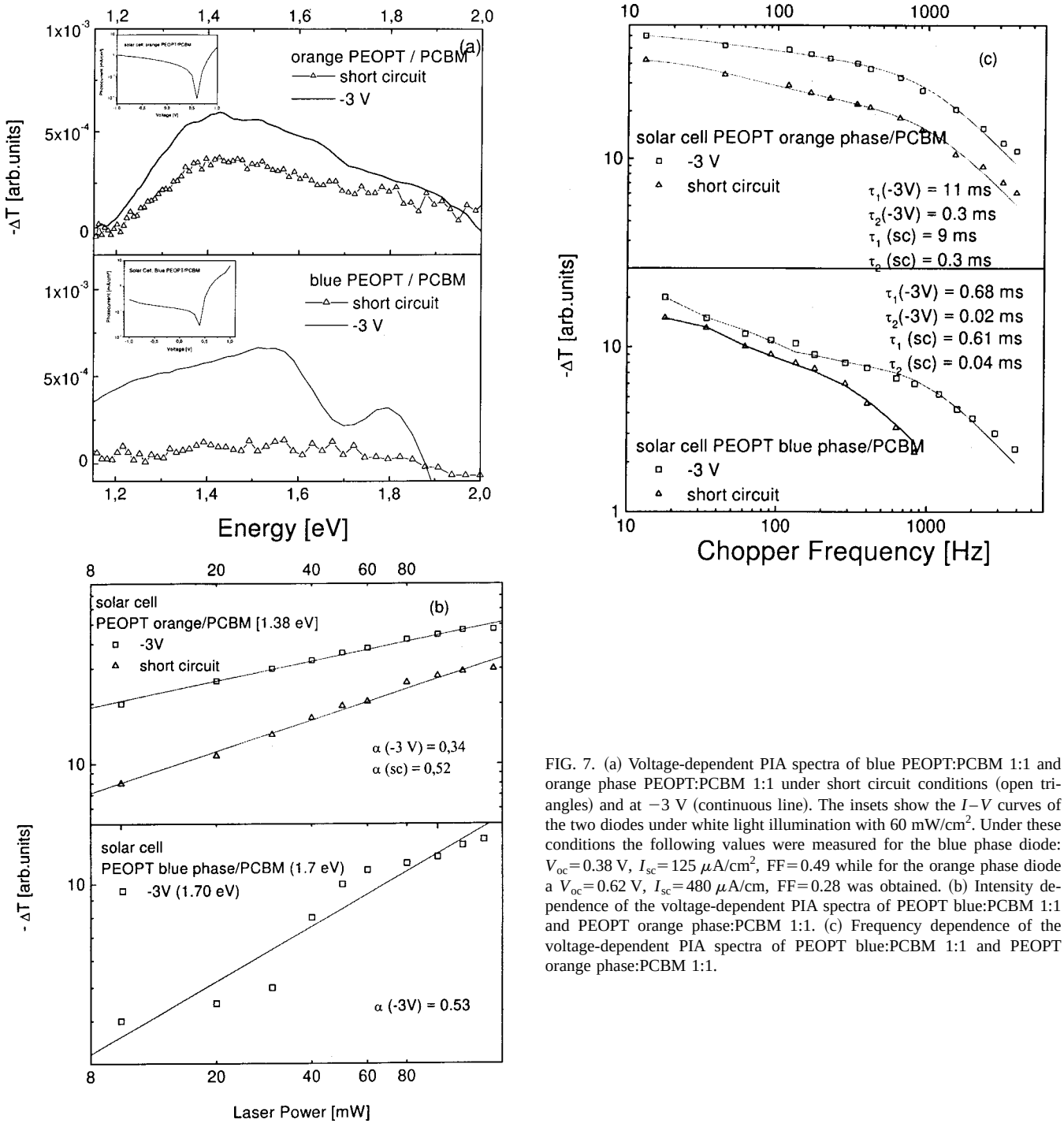

FIG. 7. (a) Voltage-dependent PIA spectra of blue PEOPT:PCBM 1:1 and orange phase PEOPT:PCBM 1:1 under short circuit conditions (open triangles) and at -3 V (continuous line). The insets show the $I-V$ curves of the two diodes under white light illumination with 60 mW/cm^2. Under these conditions the following values were measured for the blue phase diode: $V_{oc}=0.38$ V, $I_{sc}=125\ \mu$A/cm^2, FF$=0.49$ while for the orange phase diode a $V_{oc}=0.62$ V, $I_{sc}=480\ \mu$A/cm, FF$=0.28$ was obtained. (b) Intensity dependence of the voltage-dependent PIA spectra of PEOPT blue:PCBM 1:1 and PEOPT orange phase:PCBM 1:1. (c) Frequency dependence of the voltage-dependent PIA spectra of PEOPT blue:PCBM 1:1 and PEOPT orange phase:PCBM 1:1.

7(c)], that process (i) can be neglected. In order to explain the low signal intensity of the blue phase PEOPT/PCBM diode under low field, we suggest a Langevin-type[48] recombination model, which is frequently observed in low-mobility organic semiconductors with narrow bands. A limit for the applicability of Langevin recombination is that the Coulombic capture radius r_c,

$$r_c=e^2/(4\pi\epsilon\epsilon_0 kT), \tag{2}$$

has to be comparable to the mean free path λ of the carriers in the bulk of the semiconductor.

Assuming the value for $\epsilon\sim 3$, the Coulombic capture radius is calculated with $r_c\sim 19$ nm. The average mean free path λ in conjugated polymers is typically less than 5 nm,[49] which is clearly below the Coulombic capture radius r_c, thus allowing us to use the Langevin model. In this model the recombination of nongeminate carriers may be viewed as the drift of two charges together under the action of the Coulombic field E. For convenience, the negative charge on the fullerene is supposed to be stationary and only the positive charges move with an averaged electron–hole mobility μ. Using $\lambda\sim 5$ nm, the mobility of blue and orange phase PEOPT can be estimated from[50]

$$\mu=\mathbf{e}\lambda^2/\langle\tau\rangle 3kT, \tag{3}$$

with $\langle\tau\rangle$ as the average mean free lifetime of the carriers.

Taking mean lifetimes of 10 and 1 μs for the orange and blue phase at room temperature (as estimated from the 80 K values), zero-field bulk mobility values of mobility values of 10^{-6} and 10^{-5} cm^2/V s are estimated for the orange and blue phase, respectively. According to Ref. 46 polythiophenes with strong interchain interactions (blue phase) are always expected to have a higher bulk hole mobility than polythiophenes without these two-dimensional crystallites (orange phase). The bimolecular rate constant for free-electron–hole recombination γ_{eh} (Ref. 50) is then given by

$$\gamma_{eh}=e\mu/\epsilon\epsilon_0. \tag{4}$$

From Eq. (4) it is directly seen that within the Langevin limit the bimolecular recombination rate increases linearly with the mobility. Application of high fields enhances the drift velocity and by that the mean free path of the carriers, allowing escape from the Coulombic radius. Therefore we assume that the strong voltage-dependent increase of the intensity of the PIA signal for blue but also for orange PEOPT has its origin in a bias-dependent increase of the mean free path of the positive carriers.

Blue phase PEOPT is superior compared to orange phase PEOPT with respect to mobility and spectral sensitivity of the photocurrent generation. However, the price for higher mobility is paid by a higher recombination rate of charged carriers. For the nonoptimized devices presented here, the efficient carrier recombination in blue phase PEOPT/PCBM outplays the better match to the solar spectrum as well as the higher mobility and results in an overall lower short circuit current density compared to orange phase PEOPT/PCBM composites. Therefore, blue phase PEOPT/PCBM devices have to be optimized with respect to their recombination behavior.

IV. CONCLUSION

PEOPT belongs to the class of regioregular thiophenes that can show two different phases, a low-order, more amorphous phase and a high-order, more crystalline phase with large interchain interactions. Different than other regioregular polythiophenes, these interchain interactions can be easily tuned by solution processing of the material and are only observed for the blue phase of PEOPT while they are absent for orange phase PEOPT. As such, PEOPT is a very interesting conjugated polymeric material, which allows us to investigate the role of order/disorder on the photoexcited states on one and the same material without being obscured by the differences in chemical structure as it is the case when using different materials with different crystallinity.

It is further demonstrated that the band gap of the PEOPT is lowered by the phase transition of the polymer into the higher-ordered blue phase. Photoinduced charge transfer from both phases of PEOPT to a methanofullerene PCBM is demonstrated. The lower band gap of PEOPT and the assumed higher carrier mobility makes blue phase PEOPT a promising candidate for photovoltaic devices. However, strong bimolecular recombination in thick composites of blue PEOPT with PCBM results in lower short circuit currents than those for thick film orange phase PEOPT/PCBM diodes. The origin of this enhanced recombination is found to be related to the hole mobility of the polymer chain. Further optimization of the PV photovoltaic devices in the blue phase is necessary to utilize the redshifted absorption of this material.

ACKNOWLEDGMENTS

This work is performed within the Christian Doppler Foundations dedicated laboratory on Plastic Solar Cells funded by the Austrian Ministry of Economic Affairs and Quantum Solar Energy Linz Ges. m. b. H. The work is further supported by the European Commission (JOULE III), by the ''Fonds zur Förderung der wissenschaftlichen Forschung'' of Austria (Project No. P-12680-CHE), the Magistrat Linz, the ''Land Oberösterreich'' via ETP, and the Netherlands Organization for Energy & Environment (NOVEM).

[1] *Handbook of Conducting Polymers*, edited by T. A. Skotheim (Marcel Dekker, New York, 1985), Vol. 1.
[2] M. Berggren, O. Inganäs, G. Gustafsson, J. Rasmusson, M. R. Andersson, T. Hjertberg, and O. Wennerström, Nature (London) **372**, 444 (1994).
[3] T. Granlund, M. Theander, M. Berggren, M. Andersson, A. Ruseckas, V. Sundström, G. Björk, M. Granström, and O. Inganäs, Chem. Phys. Lett. **288**, 879 (1998).
[4] Z. Bao, A. Dodabalapur, and A. J. Lovinger, Appl. Phys. Lett. **69**, 4108 (1996).
[5] L. Roman, W. Mammo, L. Petterson, M. Andersson, and O. Inganäs, Adv. Mater. **10**, 774 (1998).
[6] D. Gebeyehu, C. J. Brabec, F. Padinger, T. Fromherz, J. C. Hummelen, D. Badt, H. Schindler, and N. S. Sariciftci, Synth. Met. **118**, 1 (2001).
[7] K. Yoshino *et al.*, Jpn. J. Appl. Phys., Part 2 **27**, L716 (1988).
[8] M. J. Winokur *et al.*, Synth. Met. **28**, C419 (1989).
[9] W. R. Salaneck *et al.*, J. Chem. Phys. **89**, 4613 (1988).
[10] M. Leclerc *et al.*, J. Phys. Chem. B **101**, 10075 (1997).
[11] N. Hosaka, H. Tachibana, N. Shiga, M. Matsumoto, and Y. Tokura, Phys. Rev. Lett. **82**, 1672 (1999).
[12] R. D. McCullough and R. D. Lowe, J. Chem. Soc. Chem. Commun. **70**, 1992 (1992).
[13] H. J. Fell, E. J. Samuelsen, M. R. Andersson, J. Als-Nielsen, G. Grübel, J. Mardalen, Synth. Met. **73**, 279 (1995).
[14] K. E. Aasmundtveit, E. J. Samuelsen, W. Mammo, M. Svensson, M. R. Andersson, L. A. A. Pettersson, and O. Inganäs, Macromolecules **33**, 5481 (2000).
[15] N. S. Sariciftci, L. Smilowitz, A. J. Heeger, and F. Wudl, Science **258**, 1474 (1992).
[16] S. E. Shaheen, C. J. Brabec, F. Padinger, T. Fromherz, N. S. Sariciftci, and J. C. Hummelen, Appl. Phys. Lett. **78**, 841 (2001).
[17] G. Yu, J. Gao, J. C. Hummelen, F. Wudl, and A. J. Heeger, Science **270**, 1789 (1995).
[18] C. J. Brabec, F. Padinger, J. C. Hummelen, R. A. J. Janssen, and N. S. Sariciftci, Synth. Met. **102**, 861 (1999).
[19] C. J. Brabec, F. Padinger, N. S. Sariciftci, and J. C. Hummelen, J. Appl. Phys. **85**, 6866 (1999).
[20] M. Theander, A. Yartsev, D. Zigmantas, V. Sundström, W. Mammo, M. R. Andersson, and O. Inganäs, Phys. Rev. B **61**, 12957 (2000).
[21] M. R. Andersson, O. Thomas, W. Mammo, M. Svensson, M. Thenader, and O. Inganäs, J. Mater. Chem. **9**, 1933 (1999).
[22] J. C. Hummelen, B. W. Knight, F. Lepec, F. Wudl, J. Yao, and C. L. Wilkins, J. Org. Chem. **60**, 532 (1995).
[23] C. J. Brabec, A. Cravino, G. Zerza, N. S. Sariciftci, R. Kiebooms, D. Vanderzande, and J. C. Hummelen, J. Phys. Chem. B **105**, 1528 (2001).
[24] N. S. Sariciftci, D. Braun, C. Zhang, V. Srdanov, A. J. Heeger, G. Stucky, and F. Wudl, Appl. Phys. Lett. **62**, 585 (1993).
[25] J. J. M. Halls, C. A. Walsh, N. C. Greenham, E. A. Marseglia, R. H. Friend, S. C. Moratti, and A. B. Holmes, Nature (London) **376**, 498 (1995).
[26] L. Smilowitz, N. S. Sariciftci, R. Wu, C. Gettinger, A. J. Heeger, and F. Wudl, Phys. Rev. B **47**, 13835 (1993).
[27] B. Kraabel, J. C. Hummelen, D. Vacar, D. Moses, N. S. Sariciftci, A. J. Heeger, and F. Wudl, J. Chem. Phys. **104**, 4267 (1996).
[28] N. S. Sariciftci and A. J. Heeger, Int. J. Mod. Phys. B **8**, 237 (1994).

[29] N. S. Sariciftci, Prog. Quantum Electron. **19**, 131 (1995).
[30] X. Wei, Z. V. Vardeny, N. S. Sariciftci, and A. J. Heeger, Phys. Rev. B **53**, 2187 (1996).
[31] S. Morita, A. A. Zakhidov, and K. Yoshino, Solid State Commun. **82**, 249 (1992).
[32] K. Yoshino, X. H. Yin, S. Morita, T. Kawai, and A. A. Zakhidov, Solid State Commun. **85**, 85 (1993).
[33] S. Morita, A. A. Zakhidov, and K. Yoshino, Jpn. J. Appl. Phys., Part 2 **32**, L873 (1993).
[34] K. Yoshino, T. Akashi, K. Yoshimoto, S. Morita, R. Sugimoto, and A. A. Zakhidov, Solid State Commun. **90**, 41 (1994).
[35] L. Smilowitz, N. S. Sariciftci, R. Wu, C. Gettinger, A. J. Heeger, and F. Wudl, see Ref. 26.
[36] N. S. Sariciftci and A. J. Heeger, in *Handbook of Organic Conductive Molecules and Polymers*, edited by H. S. Nalwa (Wiley, New York, 1996), Vol. 1, pp. 414–450.
[37] B. Kraabel, C. H. Lee, D. McBranch, D. Moses, N. S. Sariciftci, and A. J. Heeger, Chem. Phys. Lett. **213**, 389 (1993).
[38] B. Kraabel, D. McBranch, N. S. Sariciftci, D. Moses, and A. J. Heeger, Phys. Rev. B **50**, 18 543 (1994).
[39] C. J. Brabec, G. Zerza, G. Cerullo, S. De Silvestri, S. Luzzati, J. C. Hummelen, and N. S. Sariciftci, Chem. Phys. Lett., **340**, 232 (2001).
[40] C. H. Lee, G. Yu, N. S. Sariciftci, D. Moses, K. Pakbaz, C. Zhang, A. J. Heeger, and F. Wudl, Phys. Rev. B **48**, 15425 (1993).
[41] V. Dyakonov, G. Zoriniants, M. C. Scharber, C. J. Brabec, R. A. J. Janssen, J. C. Hummelen, and N. S. Sariciftci, Phys. Rev. B **59**, 8019 (1999).
[42] C. J. Brabec, V. Dyakonov, N. S. Sariciftci, W. Graupner, G. Leising, and J. C. Hummelen, J. Phys. Chem. **109**, 1185 (1998).
[43] X. Wei, Z. V. Vardeny, N. S. Sariciftci, and A. J. Heeger, Phys. Rev. B **53**, 2187 (1996).
[44] Z. V. Vardeny and X. Wei, in *Handbook of Conducting Polymers*, edited by T. A. Skotheim, R. L. Elsenbaumer, J. R. Reynolds (Marcel Dekker, New York, 1998).
[45] R. Österbacka, C. P. An, X. M. Jiang, and Z. V. Vardeny, Science **287**, 839 (2000).
[46] H. Sirringhaus, P. J. Brown, R. H. Friend *et al.*, Nature (London) **401**, 685 (1999).
[47] M. Pope and C. E. Swenberg, in *Electronic Processes in Organic Crystals and Polymers* (Oxford, New York, 1999), Chaps. B. 2 and XIII B.
[48] P. Langevin, Ann. Chim. Phys. **28**, 289 (1903).
[49] M. Pope and C. E. Swenberg, in *Electronic Processes in Organic Crystals and Polymers* (Oxford, New York, 1999), Chap. IX. 9.
[50] H. A. Lorentz, *Theory of Electrons* (Dover, New York, 1952), p. 267.